

Reply to Referee#1' comments:

Thank you very much for your valuable comments and suggestions. Answers were shown below.

Reviewer #1: In this manuscript, the authors are trying to quantify and investigate the impact of unknown daytime HONO sources on the HO_x budget in the eastern coast of China. The authors should address the following issues before the Manuscript can be considered for publication.

Major concerns:

1. Page 808, lines 20 to 23:

The authors concluded that HONO photolysis reaches a maximum of 10 ppb/h while that of HO₂+NO is 9.38 ppb/h, which is very unlikely. The total OH initiation sources (including that of HONO) may contribute between 15-25% of the total OH production rates. OH production rate from HO₂+NO makes typically between 60-85% of the total OH production. HONO photolysis is an initiation source of OH and does not exceed (as a net source, after subtracting OH+NO=HONO) ~3 ppb/h as maximum (e.g., Kleffmann et al., 2005; Elshorbany et al., 2009) and can reach as high as 80% of the total OH initiation sources but NOT the total OH production rate.

(i) The major reason is that we have not subtracted OH+NO=HONO. According to your suggestions, we recalculated the net OH production rate from HONO photolysis:

$P(OH)_{HONO_{net}} = P(OH)_{HONO+h\nu} - L(OH)_{OH+NO}$, where P and L are the production and loss rates, respectively (Figs. R1 and R2). As shown in Fig. R1, when the additional HONO sources were inserted into the WRF-Chem model, the diurnal peak of $P(OH)_{HONO+h\nu}$ was 10.01 ppb h⁻¹ in Beijing, 2.63 ppb h⁻¹ in Shanghai, and 2.60 ppb h⁻¹ in Guangzhou, while the diurnal peak of $L(OH)_{OH+NO}$ was 6.90 ppb h⁻¹ in Beijing, 1.73 ppb h⁻¹ in Shanghai, and 1.54 ppb h⁻¹ in Guangzhou. The net contribution of the HONO photolysis to OH (after subtracting OH+NO=HONO) reached a maximum of 3.72 ppb h⁻¹ in Beijing, 0.89 ppb h⁻¹ in Shanghai, and 0.97 ppb h⁻¹ in Guangzhou respectively (Fig. R3), consistent with the result (3 ppb h⁻¹) of Hofzumahaus et al. (2009) mentioned above.

(ii) The revised OH budgets are shown in Table R1. The contribution of the total OH initiation sources to the total OH production rates was 19.68% in Beijing, 23.28% in Shanghai, and 13.38% in Guangzhou, in the range of 15-25% mentioned by Reviewer #1. The contribution of HO₂+NO was 61.95-73.34% of the total OH production rates (Table R1), in the range of 60-85% mentioned by Reviewer #1. Additionally, among all the OH initiation sources, HONO photolysis contributed 39.85%-71.87% of the total OH initiation sources (NOT the total OH production rate), with the largest being close to the 80% mentioned above.

(iii) **We have revised our description in the Abstract section:** “When the additional HONO sources were included, the photolysis of HONO was the second source in the OH production rate in Beijing, Shanghai and Guangzhou before 10:00 LST with a maximum of 3.72 [3.06] due to the P_{unknown} ppb h⁻¹ in Beijing, whereas the reaction of HO₂ + NO (nitric oxide) was dominated after 10:00 LST with a maximum of 9.38 [7.23] ppb h⁻¹ in Beijing.”

“The daytime average OH production rate was enhanced by 0.67 [0.64] to 4.32 [3.86] ppb h⁻¹ via the reaction of HO₂ + NO, and by 0.49 [0.47] to 1.86 [1.86] ppb h⁻¹ via the photolysis of HONO.”

We have revised our results in the section 3.4: “OH radicals are produced mainly through the reaction of HO₂ + NO, the photolysis of O₃ and HONO, and the reactions between O₃ and alkenes (Fig. 11). For case R, the predominant contribution to P(OH) [production rate of OH] was the reaction of HO₂ + NO, with a diurnal peak of 4.04 ppb h⁻¹ in Beijing, 1.52 ppb h⁻¹ in Shanghai, and 3.91 ppb h⁻¹ in Guangzhou at noon (Fig. S1a, c, e in the Supplement). The photolysis of O₃ was the second most important sources of OH, which was dominant (0.91 ppb h⁻¹ in Beijing, 0.52 ppb h⁻¹ in Shanghai, and 1.20 ppb h⁻¹ in Guangzhou) at noon (Fig. S1a, c, e). Compared with the two OH sources above, the contributions of the reactions of O₃ + alkenes, HONO photolysis and others were small, lower than 0.15 ppb h⁻¹ (Fig. S1a, c, e). When the additional HONO sources were added, the most important source was the reaction of HO₂ + NO, with a diurnal maximum conversion rate reaching 9.38 [7.23] due to the P_{unknown} ppb h⁻¹ in Beijing, 2.63 [1.15] ppb h⁻¹ in Shanghai, and 4.88 [1.43] ppb h⁻¹ in Guangzhou near noon (Fig. 11a, c, e). The photolysis of HONO became the second important source of OH in Beijing and Guangzhou before 10:00 LST, and in Shanghai before 12:00 LST; the diurnal peaks were 3.72 [3.06] ppb h⁻¹ in Beijing at 09:00 LST, 0.89 [0.62] ppb h⁻¹ in Shanghai at 11:00 LST, and 0.97 [0.78] ppb h⁻¹ in Guangzhou at 09:00 LST (Fig. 11a, c, e), which were comparable to or lower than the 3.10 ppb h⁻¹ reported by Elshorbany et al. (2009).”

“For case R, the reaction of HO₂ + NO was the major source of OH [2.78 ppb h⁻¹ (81.73% of the total daytime average production rate of OH) in Beijing, 0.73 ppb h⁻¹ (67.09%) in Shanghai, and 1.75 ppb h⁻¹ (71.54%) in Guangzhou] (Fig. 12a and Table 4). The second largest source of OH was the photolysis of O₃ [0.47 ppb h⁻¹ (13.68%) in Beijing, 0.31 ppb h⁻¹ (28.17%) in

Shanghai, and 0.62 ppb h⁻¹ (25.27%) in Guangzhou] (Table 4).”

“When the additional HONO sources were inserted into the WRF-Chem model (case R_p), the daytime average OH production rate was enhanced by 4.32 (= 7.10 – 2.78) [3.86 due to the P_{unknown}] ppb h⁻¹ in Beijing, 0.67 (= 1.40 – 0.73) [0.64] ppb h⁻¹ in Shanghai, and 0.80 (= 2.55 – 1.75) [0.68] ppb h⁻¹ in Guangzhou via the reaction of HO₂ + NO, and by 1.86 (= 1.86 – 0) [1.86] ppb h⁻¹ in Beijing, 0.50 (= 0.50 – 0) [0.50] ppb h⁻¹ in Shanghai, and 0.49 (= 0.49 – 0) [0.47] ppb h⁻¹ in Guangzhou via the photolysis of HONO, respectively (Table 4). The enhancements of the daytime average OH production rate due to the photolysis of HONO were comparable to or lower than the 2.20 ppb h⁻¹ obtained by Liu et al. (2012).”

“Overall, the net daytime production rate of RO_x was increased to 3.48 (= 2.56 + 0.71 + 0.21) [2.06 due to the P_{unknown}] from 1.20 (= 0.60 + 0.43 + 0.17) ppb h⁻¹ in Beijing, 1.09 (= 0.86 + 0.19 + 0.04) [0.45] from 0.54 (= 0.36 + 0.14 + 0.04) ppb h⁻¹ in Shanghai, and 1.52 (= 1.21 + 0.26 + 0.05) [0.58] from 0.92 (= 0.68 + 0.20 + 0.04) ppb h⁻¹ in Guangzhou (Fig. 12) due to the additional HONO sources, indicating that the RO_x source was mainly from OH production, especially via the photolysis of HONO (Tables 4, S2 and S3). This result is different from the conclusion of Liu et al. (2012) that the photolysis of HONO and oxygenated VOCs is the largest RO_x source. One of the primary reasons for this is the underestimation of anthropogenic VOCs (Wang et al., 2014). For Beijing, the net production rate of RO_x was 3.48 ppb h⁻¹, lower than the 6.60 ppb h⁻¹ from the field studies of Liu et al. (2012).”

We have revised our conclusion in the Conclusion section: “(6) When the additional HONO sources were added, the photolysis of HONO became the **second** important source of OH in Beijing and Guangzhou before 10:00 LST, and in Shanghai before 12:00 LST, with a maximum of 3.72 [3.06 due to the P_{unknown}] ppb h⁻¹ in Beijing, 0.89 [0.62] ppb h⁻¹ in Shanghai, and 0.97 [0.78] ppb h⁻¹ in Guangzhou; whereas, the reaction of HO₂ + NO was the most important source of OH, dominated in Beijing and Guangzhou after 10:00 LST and in Shanghai after 12:00 LST, with a maximum of 9.38 [7.23] ppb h⁻¹ in Beijing, 2.63 [1.15] ppb h⁻¹ in Shanghai, and 4.88 [1.43] ppb h⁻¹ in Guangzhou.

(7) The additional HONO sources, especially the P_{unknown}, accelerated the whole RO_x cycle. The daytime average OH production rates were enhanced by 4.32 [3.86 due to the P_{unknown}] ppb

h⁻¹ in Beijing, 0.67 [0.64] ppb h⁻¹ in Shanghai, and 0.80 [0.68] ppb h⁻¹ in Guangzhou via the reaction of HO₂ + NO, and by 1.86 [1.86] ppb h⁻¹ in Beijing, 0.50 [0.50] ppb h⁻¹ in Shanghai, and 0.49 [0.47] ppb h⁻¹ in Guangzhou via the photolysis of HONO. The daytime average OH loss rates were increased by 2.03 [1.92 due to the P_{unknown}] ppb h⁻¹ in Beijing, 0.58 [0.55] ppb h⁻¹ in Shanghai, and 0.65 [0.58] ppb h⁻¹ in Guangzhou via the reaction of OH + NO₂, and by 1.78 [1.64] ppb h⁻¹ in Beijing, 0.31 [0.28] ppb h⁻¹ in Shanghai, and 0.42 [0.36] ppb h⁻¹ in Guangzhou via the reaction of OH + CO.”

We have revised Figs. 11 and 12 and Table 4 in the revised Manuscript (see Figs. R3 and R8 and Table R1 in this response).

2. Hofzumahaus et al. (2009) investigated the OH budget in one of this study’s domains (PRD) and measured maximum OH production rates of about 35 and 2 ppb/h from HO₂+NO and HONO photolysis, respectively. How the authors would explain these large differences between their model results and these measurements?

(i) The contribution of HONO photolysis was revised (see the response to question 1 of Reviewer #1).

(ii) The contribution of HO₂+NO in this study was not as high as ~35 ppb h⁻¹ (Hofzumahaus’s results). The major reason is the underestimation of HO₂ in our study (Fig. R5). This underestimation was partially associated with the underestimation of anthropogenic VOCs (AVOCs) emissions (Wang et al., 2014), Wang et al. (2014) demonstrated that a 68% increase in the AVOCs emissions [the uncertainty of the AVOCs emissions could be ±68% (Zhang et al., 2009)] led to significant improvements in the HO₂. We added one case simulation (Case S in Fig. R4) by increasing the AVOCs emissions by 68%. When the AVOCs emissions were increased by 68%, the conversion rate of HO₂+NO was increased to 11.43 ppb h⁻¹ from 9.38 ppb h⁻¹ in Beijing, 3.34 ppb h⁻¹ from 2.63 ppb h⁻¹ in Shanghai, 5.78 ppb h⁻¹ from 4.88 ppb h⁻¹ in Guangzhou respectively (Fig. R4).

(iii) Although the anthropogenic VOCs emissions were increased by 68%, the simulated hourly HO₂ concentrations were still considerably underestimated by comparison with the observations in the period of July 5-25, 2006 (Fig. R5). So the contribution of HO₂+NO to OH was still lower than that (35 ppb h⁻¹) of Hofzumahaus et al. (2009). Further studies are needed for HO₂ simulations.

3. Page 808, lines 24 to 28:

What is this OH production rate, daytime mean? Even then, HONO contribution is almost similar to HO₂+NO (about 4 ppb/h). That is also very unlikely, see above. Further the loss terms due to CO is very high. If CO loss term is very high in the region, you would probably have also so much VOC loss and therefore also high HO₂+NO to compensate, given the high NO_x levels in eastern China.

(i) We used *“the daytime average OH production rate”* instead of *“the OH production rate”*, and used *“the daytime average OH loss rate”* instead of *“the OH loss rate”*, and added necessary *“daytime average”* in the whole revised version.

(ii) After recalculating the net OH production rate from HONO photolysis (subtracting OH+NO=HONO), the contribution of HO₂+NO to the OH production rate was much higher than that of HONO photolysis (Fig. R3). The former reached a maximum of 9.38 ppb h⁻¹ in Beijing, 2.63 ppb h⁻¹ in Shanghai, and 4.88 ppb h⁻¹ in Guangzhou, respectively, while the maximum of the later was 3.72 ppb h⁻¹ in Beijing, 0.89 ppb h⁻¹ in Shanghai, and 0.97 ppb h⁻¹ in Guangzhou, respectively (Fig. R3).

(iii) The contribution of HO₂+NO in this study was not high. The major reason is the underestimation of HO₂ in our study (see the response to question 2 of Reviewer#1).

4. Page 813, line 13:

By referring to the mentioned study, it is HONO/NO_x and not HONO/NO₂.

We have revised our description in the Introduction section: *“This is the reason why the recent CalNex 2010 (California Research at the Nexus of Air Quality and Climate Change) study found a very strong positive correlation ($R^2 = 0.985$) between HONO flux and the product of NO₂ concentration and solar radiation at Bakersfield site (Ren et al., 2011).”*

5. Page 813, line 17:

The authors mentioned they used data from 13 field measurement campaigns around the globe. Why data from around the globe if the study domain is located only on eastern coast of China?

We used the data from 13 field measurement campaigns around the globe. The reasons are below:

(i) We want to know whether the correlations of the P_{unknown} with NO₂ mixing ratios and [NO₂] J(NO₂) are consistent around the globe.

(ii) The measurement campaigns of HONO are still limited around the world, especially in China, but a statistical result needs large samples.

(iii) Fig. R6 shows the correlations of the P_{unknown} with [NO₂] and [NO₂] J(NO₂) in the coastal

areas of China, the other countries, and the globe, respectively. Compared with that around the globe (Fig. R6ef), the correlation coefficient (R^2) between the P_{unknown} and $[\text{NO}_2]$ was decreased to 0.38 from 0.75, while the correlation coefficient between the P_{unknown} and $[\text{NO}_2] \cdot J(\text{NO}_2)$ was decreased to 0.48 from 0.80 (Fig. R6abef). However, the linear regression slope of the latter was 17.37 (Fig. R6b), very close to the 19.60 based on the data around the globe (Fig. R6f).

The correlation coefficients between the P_{unknown} and $[\text{NO}_2]$ and between the P_{unknown} and $[\text{NO}_2] \cdot J(\text{NO}_2)$ were 0.15 and 0.33, respectively (Fig. R6cd), much lower than those in the coastal areas of China (Fig. R6ab).

(iv) The description was added in section 2.2: *“For the coastal regions of China, the correlation between the P_{unknown} and $[\text{NO}_2] \cdot J(\text{NO}_2)$ was 0.48, with a linear regression slope of 17.37 (Fig. S2b in the Supplement), which is within the maximum P_{unknown} uncertainty range of 25% (Table S1).”*

(v) The uncertainties in the observed data were added in the Table R2. In the study of Su et al. (2008, 2011), the uncertainty in the P_{unknown} values calculated by the PSS (see the response to question 8 of Reviewer #1) is 10-25%. Sörgel et al. (2011) suggested the uncertainty in the PSS mainly originated from OH measurements with an accuracy of $\pm 18\%$. With the same method (PSS), Wong et al. (2012) also proposed an uncertainty of 10-20% in the P_{unknown} values. To assess the impacts of the uncertainty in the P_{unknown} parameterization on production and loss rates of HONO, two sensitivity cases (Case R_{inc} and Case R_{dec}) were performed. Case R_{inc} includes case R_p with an increase of 25% (the maximum uncertainty range according to the previous studies above) in the slope factor (19.60); Case R_{dec} is the same as case R_p with a decrease of 25% in the slope factor (19.60). The sensitivity results show that a 25% increase (25% decrease) in the slope factor (19.60) led to a 9.19-18.62% increase (12.69-14.32% decrease) in the maximum HONO production rate and a 0-17.64% increase (8.40-14.07% decrease) in the maximum HONO loss rate (Fig.R7) (section 3.2 in the revised version). The uncertainty analysis were added in the section 3.2: *“The maximum P_{unknown} uncertainty range of 25% (Table S1), a 25% increase (decrease) in the slope factor (19.60) led to a 9.19–18.62% increase (12.69–14.32% decrease) in the maximum HONO production rate*

and a 0–17.64% increase (8.40–14.07% decrease) in the maximum HONO loss rate (Fig. S3 in the Supplement).”

6. Page 815, line 1:

Which studies? Please write the reference(s).

The references were added in section 2.2: “*Previous studies (Sörgel et al., 2011; Villena et al., 2011; Wong et al., 2012) have shown $P_{\text{unknown}} \propto [\text{NO}_2] J(\text{NO}_2)$.*”

7. Page 815, line 5:

Figure 2 is not clear at all; references are almost not readable. Which good correlation the authors mean? The slope and the correlation coefficient in these two plots are calculated based on the high NO₂ points! The low NO₂ points do not correlate at all and should have been plotted in another plot? And would have probably results in negative slope.

(i) **The data and related references used in Figure 2 were added in Table R2 (were also added in the revised Supplement).**

(ii) According to your suggestions, we calculated the correlations of the P_{unknown} with [NO₂] and [NO₂] J(NO₂) in China (corresponding to the high NO₂ points) and in the other countries (corresponding to the low NO₂ points) as shown in Fig. R6. Please see the response to question 5 of Reviewer #1, the correlation coefficients calculated based on the high NO₂ points located mainly in China were higher than those based on the low NO₂ points located mainly in the other countries.

8. Also, How the authors define the data selection criteria (for Fig 2), e.g., did the authors used J-values near sunrise and sunset? What type of data (mean, median, max, min, ..etc.), measurements techniques, ..etc..?

Please see Table R2.

(i) The P_{unknown} in this study was calculated by the daytime HONO budget analysis below.

$$\frac{d[\text{HONO}]}{dt} = (P_{\text{OH} + \text{NO}} + P_{\text{emission}} + P_{\text{transport}} + P_{\text{unknown}}) - (L_{\text{HONO} + \text{hv}} + L_{\text{OH} + \text{HONO}} + L_{\text{deposition}} + L_{\text{transport}})$$

(Sörgel et al., 2011; Wong et al., 2012; Spataro et al., 2013)

where $\frac{d[\text{HONO}]}{dt}$ is the instantaneous rate of HONO, $P_{\text{OH}+\text{NO}}$ is HONO production rate

from R1, $P_{\text{transport}}$ is HONO transport processes including horizontal and vertical transports,

P_{emission} is direct emissions of HONO from vehicles, P_{unknown} is the additional unknown

daytime HONO source(s). In the sink terms, $L_{\text{HONO}+\text{hv}}$ is HONO photolysis rate, $L_{\text{HONO}+\text{OH}}$ is

HONO loss rate by HONO+OH, $L_{\text{deposition}}$ is HONO deposition rate, and $L_{\text{transport}}$ is dilution

effects through transport processes. When the photolysis frequency of HONO (J_{HONO}) is

greater than $1.0 \times 10^{-3} \text{ s}^{-1}$, the lifetime of HONO is less than 17 minutes. Then the influences of transport and deposition on HONO ($P_{\text{transport}}$, $L_{\text{deposition}}$ and $L_{\text{transport}}$) are weak, can be omitted from the equation above. Therefore, the equation could be expressed:

$$P_{\text{unknown}} + P_{\text{OH} + \text{NO}} + P_{\text{emission}} \approx L_{\text{HONO} + \text{hv}} + L_{\text{OH} + \text{HONO}}$$

To obtain reasonable P_{unknown} values, we must ensure that all of $J(\text{NO}_2)$ values we used are higher than $1.0 \times 10^{-3} \text{ s}^{-1}$. The data used in this study were in the daytime (from 8:00 to 15:30), and the $J(\text{NO}_2)$ values near sunrise and sunset were eliminated (Table R2).

(ii) Mean values of the data were used, and related references as well as the measurement techniques were added in Table R2.

9. Since the study of the impact of the unknown HONO sources is limited to China, why do not you limit the analysis and the parameterization to these regions. This way, the authors would be able to better parameterize this unknown source, given the knowledge of all controlling factors, e.g., surface areas, topography, radiation and dynamics. Limiting the parameterization to the measurement location would also help elucidate and shed some light on the sources and nature of this unknown source.

(i) Although our studied areas are focused on the coastal areas of China, very useful is a general parameterization of the P_{unknown} used in different regions of the world. For the correlation between the P_{unknown} and $[\text{NO}_2] J(\text{NO}_2)$ the linear regression slope was 17.37 in China (Fig. R6b), very close to the value of 19.60 around the globe (Fig. R6f), indicating that the P_{unknown} parameterization can be used in different regions of the world, where NO_x emissions are high.

(ii) Your suggestions are very important. However, some controlling factors, e.g., measured surface areas and radiation are not available from the references (Wu et al., 2013, Villena et al., 2011, N. Zhang et al., 2012,) (Table R2), except for Su et al. (2011) and Spataro et al. (2013); Your suggestions will be considered in the future.

10. The authors need to first determine the correct parameterization for this region before investigating the impacts on HO_x , which would also require reasonable estimation of HO_x budgets. According to your suggestions, we have shown the details about the parameterization for China and other countries (see above).

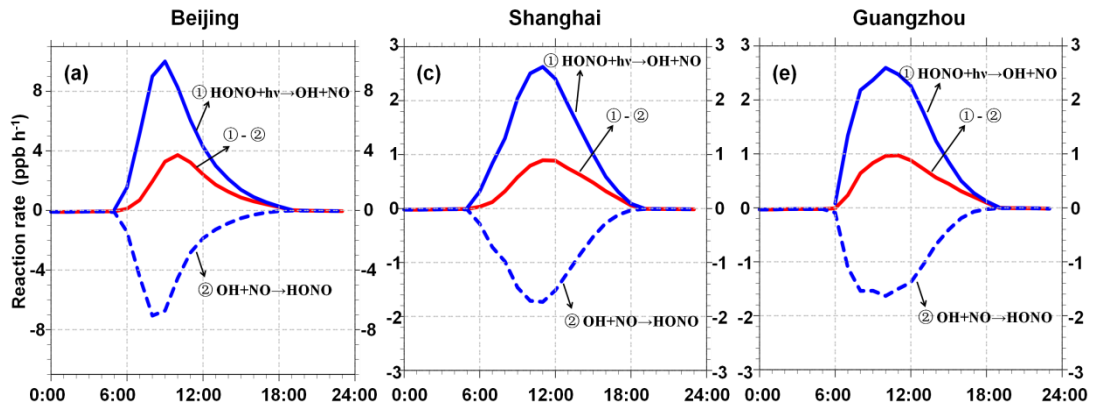


Fig. R1 Averaged reaction rates of $\text{HONO} + \text{h}\nu \rightarrow \text{OH} + \text{NO}$ (①), and $\text{OH} + \text{NO} \rightarrow \text{HONO}$ (②), and the net OH production rate by HONO photolysis (①-②) for case R_p in (a) Beijing, (b) Shanghai, and (c) Guangzhou in August 2007.

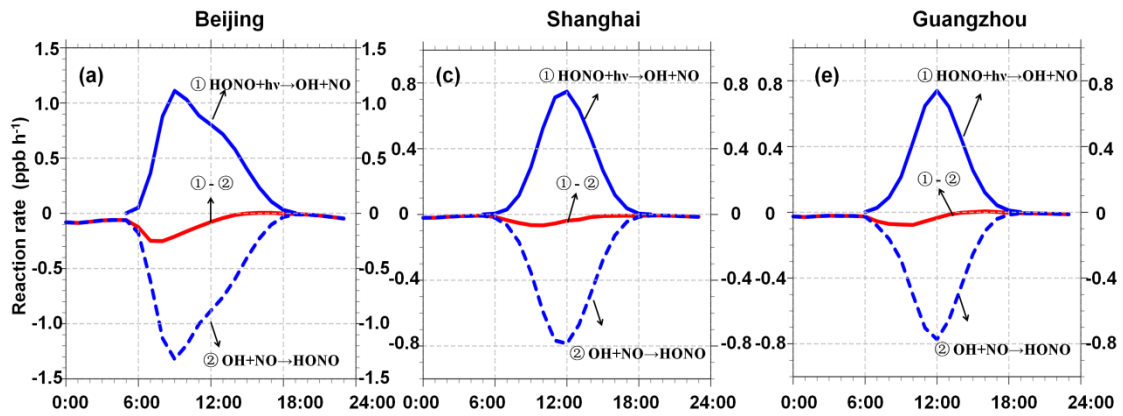


Fig. R2 Averaged reaction rates of $\text{HONO} + \text{h}\nu \rightarrow \text{OH} + \text{NO}$ (①), and $\text{OH} + \text{NO} \rightarrow \text{HONO}$ (②), and the net OH production rate by HONO photolysis (①-②) for case R in (a) Beijing, (b) Shanghai, and (c) Guangzhou in August 2007.

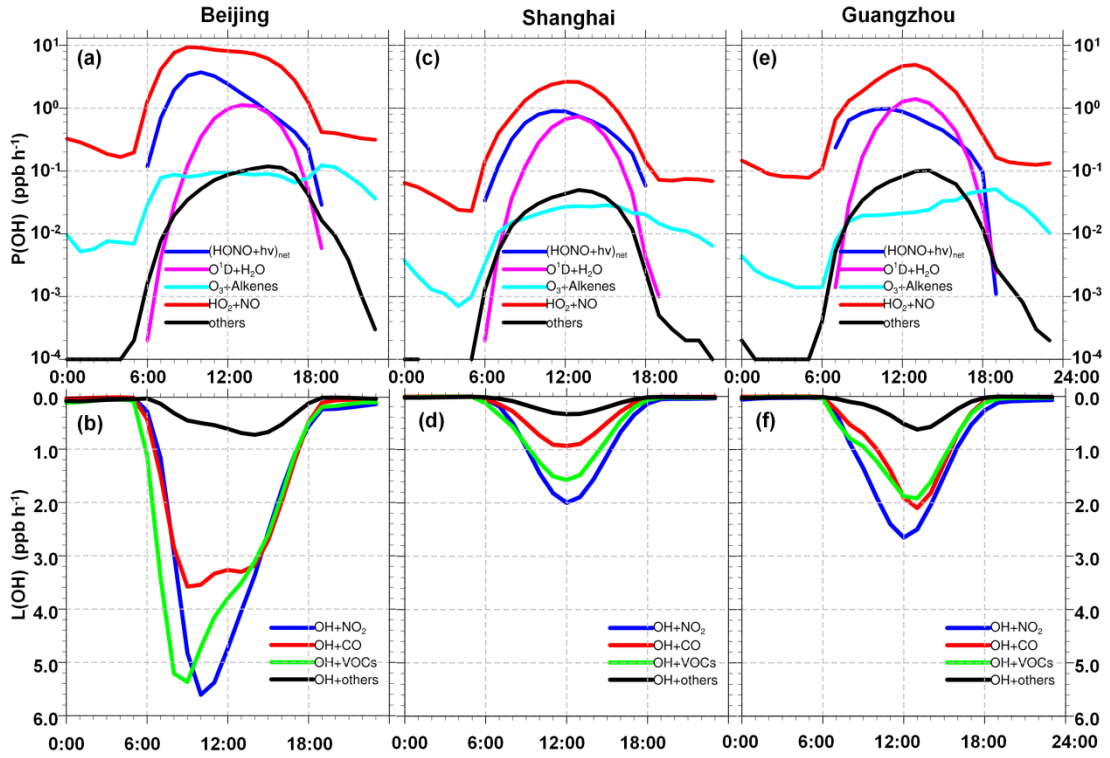


Fig. R3. Averaged production [P(OH)] and loss [L(OH)] rates of OH for case R_p in (a, b) Beijing, (c, d) Shanghai, and (e, f) Guangzhou in August 2007. $(\text{HONO}+h\nu)_{\text{net}}$ means the net OH production rate from HONO photolysis (subtracting $\text{OH} + \text{NO} = \text{HONO}$).

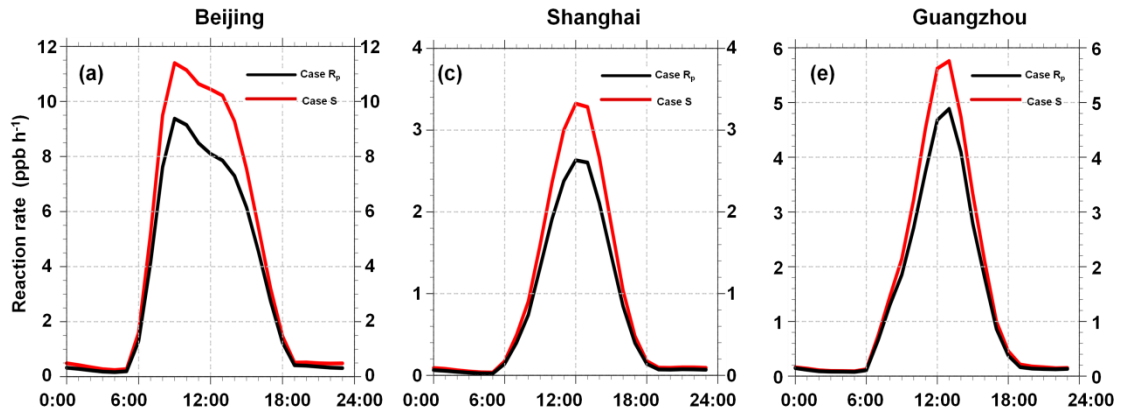


Fig. R4. Comparison of averaged conversion rates of HO_2 to OH between case R_p and case S (increasing the anthropogenic VOCs emissions by 68%) in (a) Beijing, (b) Shanghai, and (c) Guangzhou in August 2007.

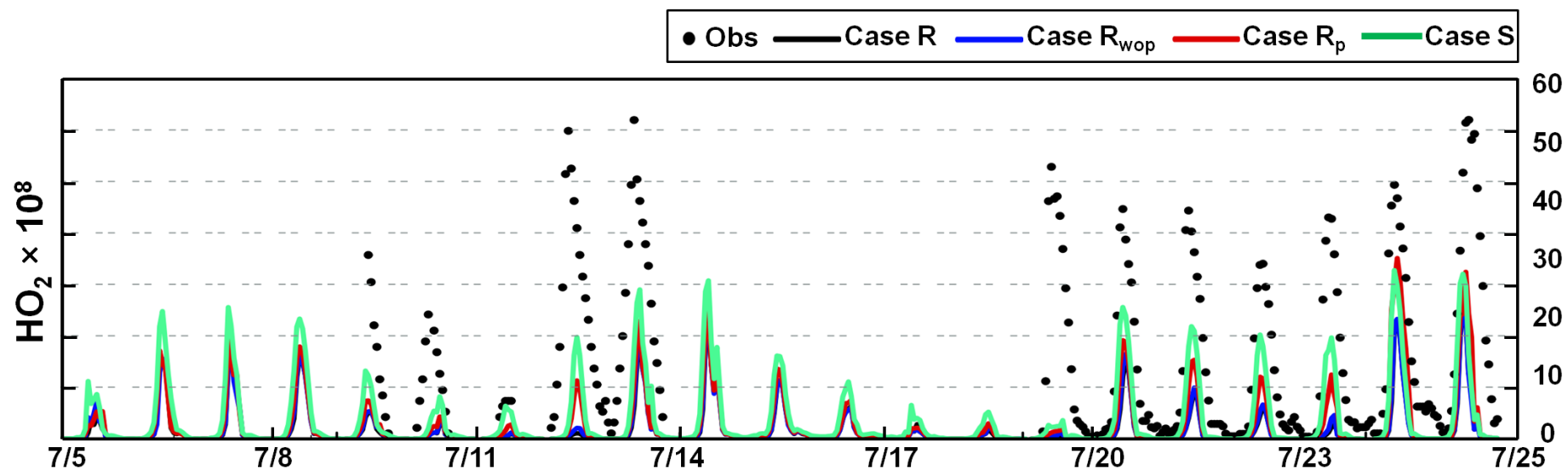
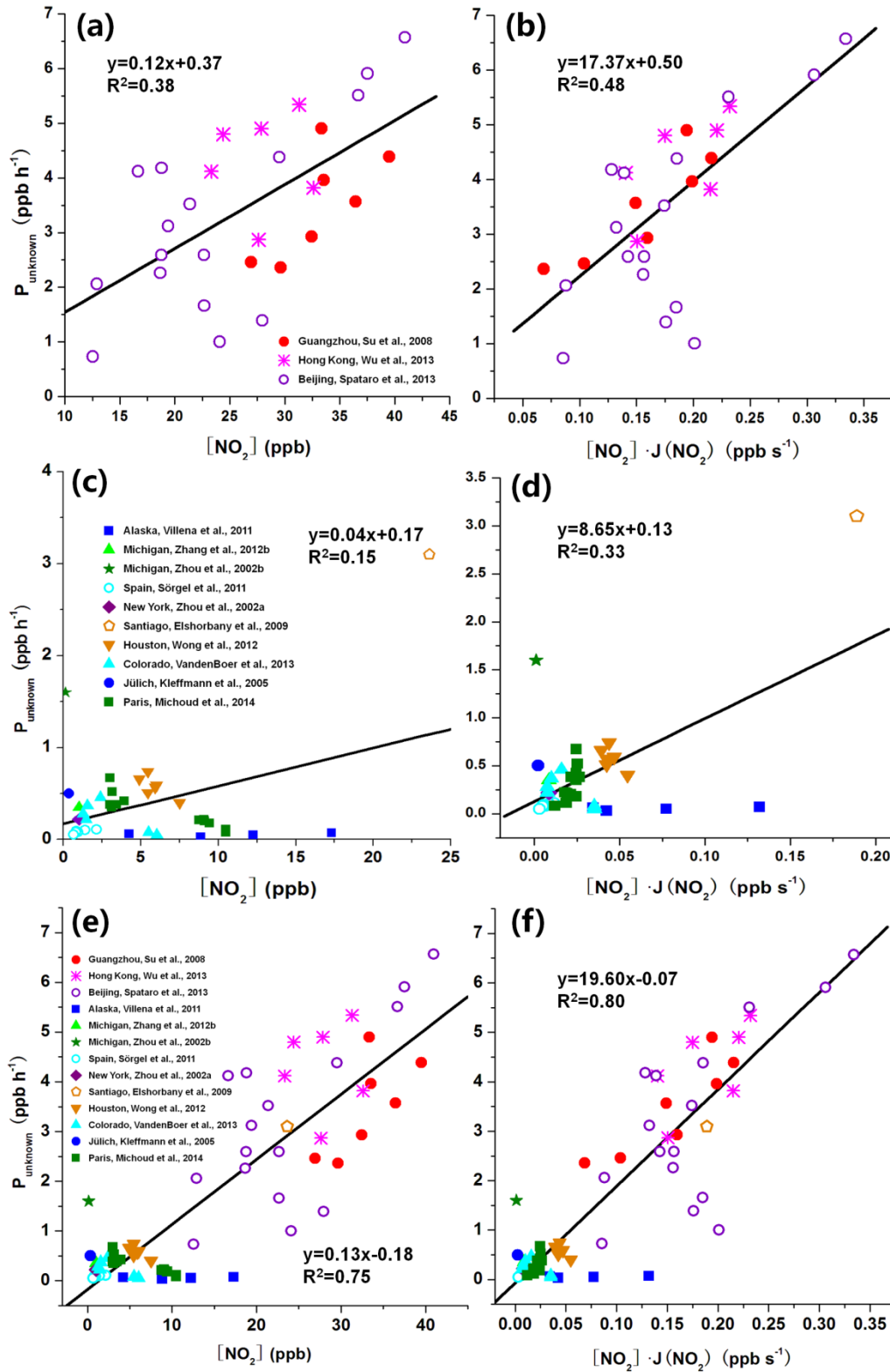
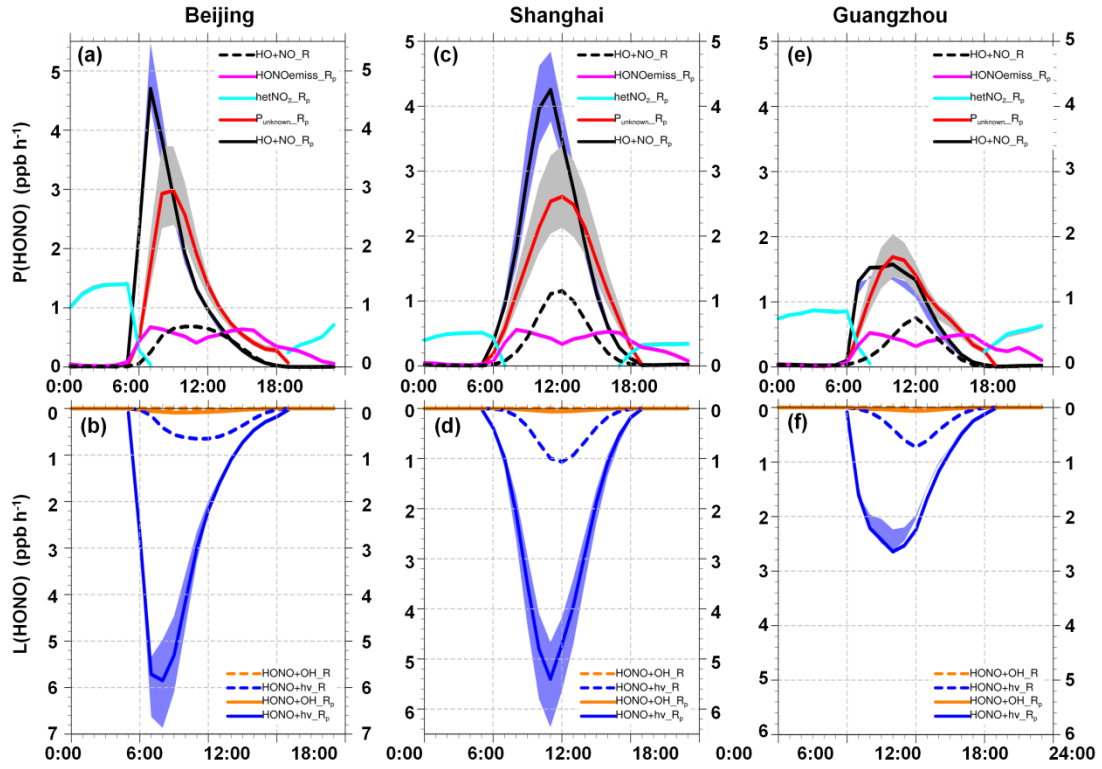


Fig. R5. Comparison of simulated and observed hourly-mean mixing ratios of HO_2 (molecules cm^{-3}) at the Backgarden site in Guangzhou in July 2006 (Lu et al., 2012). (Case S: a 68% increase in the anthropogenic emissions of VOCs for Case R_p).



1

2 Fig. R6. Correlations of the unknown daytime HONO source (P_{unknown}) (ppb h^{-1}) with NO_2 mixing
 3 ratios (ppb) and $[\text{NO}_2] \cdot J(\text{NO}_2)$ (ppb s^{-1}) in (a), (b) the coastal regions of China, (c), (d) the other
 4 countries, and (e), (f) the globe, respectively, based on the field experiment data shown in Fig. 1 in
 5 the revised version.



6

7

8 Fig. R7. Production [$P(\text{HONO})$] and loss [$L(\text{HONO})$] rates of HONO for cases R (dashed lines),

9 R_p (solid lines) and sensitivity ranges (based on R_{inc} and R_{dec}) in (a), (b) Beijing, (c), (d) Shanghai,

10 and (e), (f) Guangzhou in August 2007. Case R_{inc} includes case R_p with an increase of 25% (the

11 maximum uncertainty range according to the previous studies above) in the slope factor (19.60);

12 Case R_{dec} is the same as case R_p with a decrease of 25% in the slope factor (19.60).

13

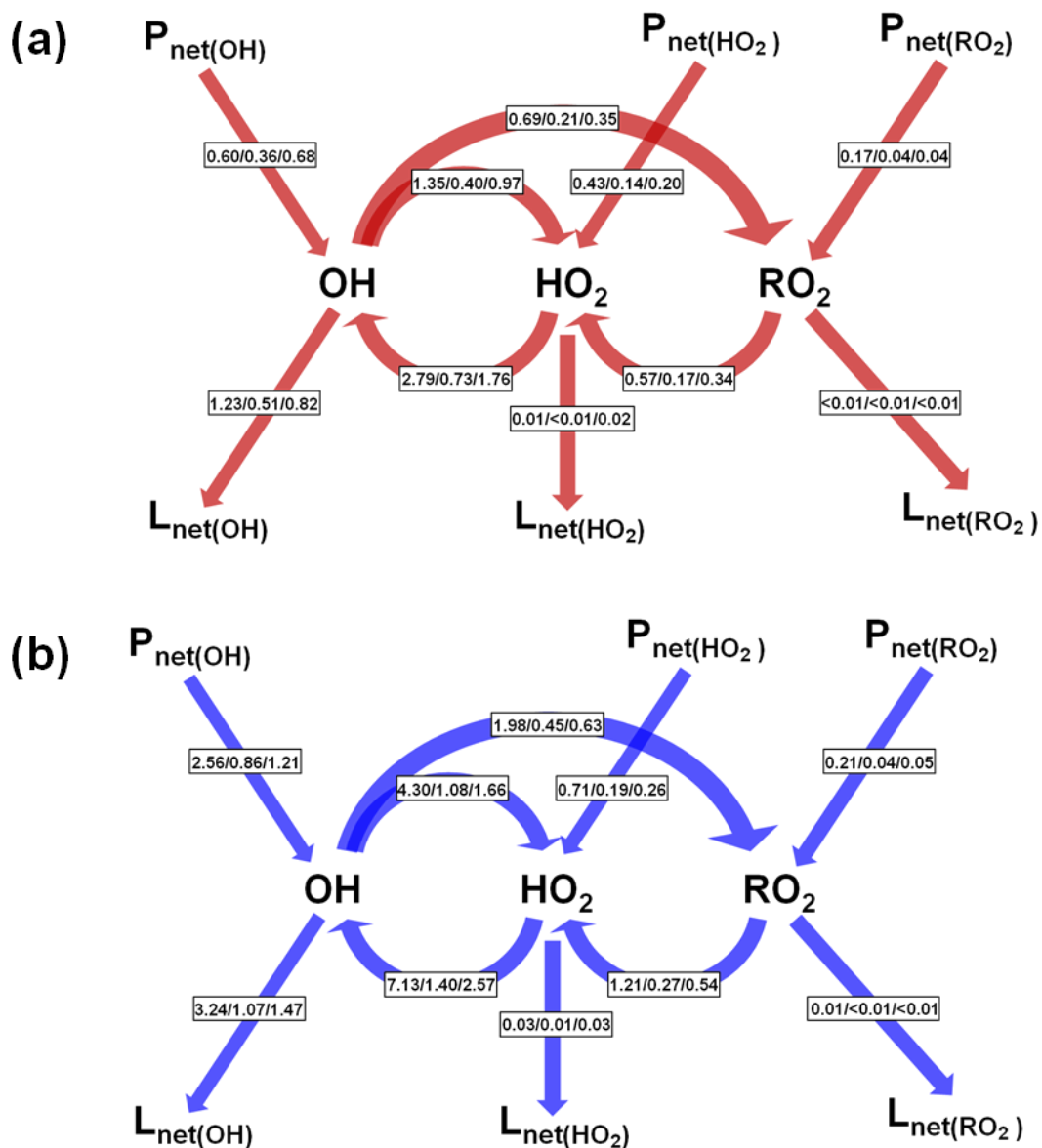
14

15

16

17

18



19

20 Fig. R8. Daytime (06:00–18:00 LST) average budgets of OH, HO₂ and RO₂ radicals (reaction

21 rates, ppb h⁻¹) for cases (a) R and (b) R_p in Beijing/Shanghai/Guangzhou in August 2007.

22
23
24
25
26
27
28
29
30

Table R1. Daytime (06:00–18:00 LST) average OH budgets in Beijing/Shanghai/Guangzhou in August 2007.

Reaction	Case R		Case R _{wop}		Case R _p	
	Rate (ppb h ⁻¹)	Contribution (%)	Rate (ppb h ⁻¹)	Contribution (%)	Rate (ppb h ⁻¹)	Contribution (%)
OH production						
HO₂+NO	2.778/0.732/1.748	81.73/67.09/71.54	3.242/0.760/1.871	83.74/68.00/72.02	7.101/1.402/2.553	73.34/61.95/67.55
* (HONO+hv)_{net}	--/--/--	--/--/--	--/--/0.017	--/--/0.66	1.855/0.497/0.489	19.16/21.98/12.93
O¹D+H₂O	0.465/0.307/0.617	13.68/28.17/25.27	0.479/0.306/0.630	12.36/27.38/24.24	0.568/0.312/0.651	5.86/13.80/17.23
O ₃ +OLET/OLEI	0.101/0.024/0.027	2.98/2.16/1.11	0.095/0.023/0.027	2.45/2.08/1.03	0.080/0.021/0.025	0.83/0.91/0.65
* (H₂O₂+hv)_{net}	0.035/0.023/0.029	1.02/2.07/1.17	0.035/0.023/0.030	0.91/2.03/1.16	0.037/0.022/0.032	0.38/0.97/0.19
HO ₂ +O ₃	0.009/0.001/0.014	0.28/0.07/0.59	0.010/0.001/0.015	0.26/0.06/0.58	0.026/0.001/0.019	0.27/0.05/0.51
* (HNO₃+hv)_{net}	0.005/0.001/0.002	0.15/0.06/0.10	0.005/0.001/0.002	0.13/0.06/0.09	0.007/0.001/0.003	0.07/0.04/0.07
ROOH+hv	0.003/0.004/0.005	0.09/0.36/0.19	0.003/0.004/0.005	0.09/0.38/0.19	0.007/0.007/0.007	0.07/0.29/0.19
O ₃ +ETH	0.002/<0.001/<0.001	0.05/0.02/0.01	0.002/<0.001/<0.001	0.04/0.02/0.01	0.001/<0.001/<0.001	0.02/0.01/0.01
HO ₂ +NO ₃	<0.001/<0.001/<0.001	<0.01/<0.01/0.01	<0.001/<0.001/<0.001	<0.01/<0.01/<0.01	<0.001/<0.001/<0.001	<0.01/<0.01/<0.01
O ₃ +ISOP	<0.001/<0.001/<0.001	0.01/<0.01/<0.01	<0.001/<0.001/<0.001	0.01/<0.01/<0.01	<0.001/<0.001/<0.001	<0.01/<0.01/<0.01
Total	3.399/1.091/2.443	100/100/100	3.873/1.118/2.598	100/100/100	9.683/2.263/3.779	100/100/100
OH loss						
OH+NO₂	1.116/0.474/0.770	39.31/46.63/38.33	1.225/0.501/0.844	38.11/45.86/38.86	3.146/1.045/1.424	38.08/44.29/40.76
OH+CO	0.785/0.203/0.576	27.65/19.97/28.67	0.932/0.227/0.637	29.00/20.78/29.33	2.573/0.506/1.001	31.14/21.45/28.65
OH+OLET/OLEI	0.192/0.054/0.059	6.76/5.31/2.94	0.264/0.065/0.077	8.21/5.95/3.55	0.537/0.206/0.095	6.50/8.73/2.72
OH+HCHO	0.150/0.050/0.146	5.28/4.92/7.27	0.166/0.053/0.156	5.16/4.85/7.18	0.544/0.096/0.242	6.59/4.07/6.93
OH+CH ₄	0.103/0.057/0.135	3.63/5.61/6.72	0.109/0.059/0.142	3.39/5.40/6.54	0.260/0.115/0.223	3.15/4.87/6.38
OH+ALD2/MGLY/AN OE	0.092/0.018/0.045	3.24/1.77/2.24	0.109/0.020/0.049	3.39/1.83/2.26	0.323/0.047/0.081	3.91/1.99/2.32
OH+SO ₂	0.054/0.030/0.035	1.90/2.95/1.74	0.064/0.034/0.041	1.99/3.11/1.89	0.172/0.116/0.072	2.08/4.92/2.06

OH+XYL	0.052/0.022/0.023	1.83/2.16/1.14	0.066/0.026/0.029	2.05/2.38/1.34	0.141/0.078/0.045	1.71/3.31/1.29
OH+H ₂	0.038/0.021/0.050	1.34/2.07/2.49	0.040/0.022/0.052	1.24/2.01/2.39	0.095/0.027/0.075	1.15/1.14/2.15
OH+TOL	0.027/0.007/0.011	0.95/0.69/0.55	0.034/0.008/0.014	1.06/0.73/0.64	0.086/0.025/0.024	1.04/1.06/0.69
OH+HONO	0.003/0.003/0.005	0.11/0.30/0.25	0.006/0.004/0.007	0.19/0.37/0.32	0.069/0.023/0.032	0.84/0.97/0.92
OH+HNO _x	0.005/0.001/0.005	0.18/0.10/0.25	0.005/0.001/0.005	0.16/0.09/0.23	0.015/0.002/0.008	0.18/0.08/0.23
OH+O ₃	0.028/0.006/0.035	0.99/0.59/1.70	0.029/0.006/0.036	0.90/0.55/1.66	0.072/0.005/0.046	0.87/0.21/1.32
OH+H ₂ O ₂	0.015/0.008/0.027	0.53/0.79/1.34	0.016/0.008/0.029	0.50/0.73/1.34	0.040/0.010/0.043	0.48/0.42/1.23
OH+ETH/OPEN	0.007/0.002/0.004	0.25/0.20/0.20	0.008/0.002/0.005	0.25/0.18/0.23	0.036/0.009/0.011	0.44/0.38/0.31
OH+CH ₃ OOH/ROOH	0.010/0.011/0.014	0.35/1.08/0.70	0.011/0.012/0.014	0.34/1.10/0.64	0.022/0.020/0.022	0.27/0.85/0.63
OH+ISOP	0.019/0.004/0.002	0.67/0.39/0.10	0.020/0.004/0.003	0.62/0.37/0.14	0.017/0.007/0.003	0.21/0.30/0.09
OH+PAR	0.005/0.002/0.004	0.18/0.20/0.20	0.007/0.003/0.005	0.22/0.27/0.23	0.015/0.005/0.007	0.18/0.21/0.20
OH+ONIT /ISOPRD	0.028/0.005/0.016	0.99/0.49/0.80	0.030/0.005/0.018	0.93/0.46/0.83	0.077/0.013/0.025	0.93/0.55/0.72
OH+C ₂ H ₆	0.002/0.001/0.002	0.07/0.10/0.10	0.003/0.001/0.002	0.09/0.09/0.09	0.008/0.002/0.004	0.10/0.08/0.11
OH+CH ₃ OH/ANOL/C RES	0.002/0.001/0.002	0.07/0.10/0.10	0.002/0.001/0.002	0.06/0.09/0.09	0.007/0.002/0.003	0.08/0.08/0.09
OH+HO ₂	0.001/<0.001/0.004	0.04/0.05/0.20	0.002/<0.001/0.005	0.06/0.05/0.23	0.006/<0.001/0.008	0.07/0.02/0.23
OH+NO	0.105/0.036/0.039	3.70/3.54/1.94	0.066/0.030/--	2.05/2.75/--	--/--/--	--/--/--
Total	2.839/1.017/2.009	100/100/100	3.214/1.093/2.172	100/100/100	8.261/2.360/3.495	100/100/100

OLET: internal olefin carbons (C=C); OLEI: terminal olefin carbons (C=C); ROOH: higher organic peroxide; ETH: ethene; ISOP: isoprene;

ALD2: acetaldehyde; MGLY: methylglyoxal; ANOE: acetone; XYL: xylene; TOL: toluene; HNO_x: HNO₃ + HNO₄; OPEN: aromatic fragments;

PAR: paraffin carbon -C-; ONIT: organic nitrate; ISOPRD: lumped intermediate species; ANOL: ethanol; CRES: cresol and higher molar weight phenols.

Table R2. The calculated unknown daytime HONO source (P_{unknown}), NO_2 mixing ratios and photolysis frequency of NO_2 [$J(\text{NO}_2)$] from field experiments in Figure 1.

Site	Date	Time	P_{unknown} (ppb h^{-1})	$[\text{NO}_2]$ (ppb)	$J(\text{NO}_2)$ ($\times 10^{-3} \text{ s}^{-1}$)	Measurement techniques /Uncertainties	Reference
Xinken (22.6 N, 113.6 E)	2004.10.23- 2004.10.30	09:30	2.36	29.65	2.31	HONO: WD/IC;	Su et al. (2008) Su et al. (2011)
		10:30	3.57	36.46	4.09	NO_2 : estimated from NO and NO_y	
		11:30	4.39	39.51	5.46	(measured by the NO- O_3	
		12:30	4.90	33.33	5.83	chemiluminescence detector (Kondo et	
		13:30	3.96	33.54	5.93	al., 1997))/22%;	
		14:30	2.93	32.43	4.92	$J(\text{NO}_2)$: TUV/18%;	
		15:30	2.46	26.94	3.85	P_{unknown} : 10~30%.	
Beijing (39.99 N, 116.30 E)	2007.08.17	8:00	2.59	22.66	6.29		Spataro et al. (2013)
		10:00	1.66	22.67	8.16		
		12:00	1.00	24.09	8.35		
		14:00	3.12	19.39	6.82	HONO: Annular denuders;	
	2007.08.18	8:00	1.39	27.96	6.29	NO_2 : means of commercial ECOTECH	
		10:00	3.52	21.37	8.16	Ltd. (Australia analyzer)/ 1%;	
		12:00	4.12	16.66	8.35	$J(\text{NO}_2)$: calculated by $J(\text{HONO})$;	
		14:00	2.06	12.90	6.82		
	2007.08.19	8:00	4.38	29.50	6.29		
		10:00	5.91	37.53	8.16		
		12:00	2.26	18.67	8.35		

		14:00	0.73	12.54	6.82		
		8:00	5.51	36.69	6.29		
	2007.08.20	10:00	6.57	40.94	8.16		
		12:00	2.59	18.78	8.35		
		14:00	4.18	18.79	6.82		
		10:00	2.87	27.62	5.45		
Tung Chung		11:00	3.82	32.62	6.59	HONO: LOPAP;	
(22.30 N,	2011.08.25-	12:00	5.34	31.31	7.41	NO ₂ : TEI;	
113.93 E)	2011.08.31	13:00	4.90	27.86	7.92	J(NO ₂): Optical actinometer.	Wu et al. (2013)
		14:00	4.80	24.40	7.17		
		15:00	4.12	23.33	6.02		
		10:30	0.03	-	4.73		
		11:00	0.03	-	6.03	HONO: LOPAP;	
		11:30	0.06	4.23	8.16	NO ₂ : estimated from NO and NO _y	
Alaska		12:00	0.09	-	8.81	(measured by the NO-O ₃	
(71.32 N,	2009.03.13-	12:30	0.05	-	9.46	chemiluminescence detector;	Villena et al. (2011)
156.65 W)	2009.04.14	13:00	0.08	-	8.69	J(NO ₂): estimated as a function of solar	
		13:30	0.07	17.31	7.63	zenith angle using the TUV radiative	
		14:00	0.05	12.24	6.33	transfer model.	
		14:30	0.03	8.85	4.79		
Michigan	2008.07.17-	noon	0.35	1.00	8.48	HONO: LOPAP;	
(45.50 N,	2008.08.07					NO ₂ : Custom-built analyzer using the	N. Zhang et al. (2012)

84.70 °W)							chemiluminescence technique; J(NO ₂): estimated as a function of UV measured by the TUV radiative transfer model/10%.	
Michigan (45.50 N, 84.70 °W)	2000.07.27	noon	1.60	0.13	8.48		HONO: Two-channel measurement system (Zhou et al., 1999); NO ₂ : TEI Model.	Zhou et al. (2002a)
		10:00	0.11	2.15	5.39			
		11:00	0.10	1.38	6.26		HONO: LOPAP/12%;	
Spain (37.10 N, 6.74 °W)	2008.07.17- 2008.08.07 (cloud-free)	12:00	0.08	0.95	6.76		NO ₂ : Droplet Measurement Technologies (Hosaynali-Beygi et al., 2011)/8%;	Sörgel et al. (2011)
		13:00	0.09	0.84	6.68		J(NO ₂): Filter radiometers/5%;	
		14:00	0.08	0.79	6.03		P _{unknown} : 18%.	
		15:00	0.05	0.66	4.62			
New York (42.09 N, 77.21 °W)	1998.06.26- 1998.07.14	noon	0.22	1.00	8.48		HONO: Two-channel measurement system (Zhou et al., 1999); NO ₂ : TEI Model.	Zhou et al. (2002b)
Santiago (33.45 S, 70.67 °W)	2005.03.08- 2005.03.20	noon	1.70	10.00	8.00		HONO: LOPAP; NO ₂ : DOAS-OPIS optical system; J(NO ₂): Filter radiometers.	Elshorbany et al. (2009)
Houston (29.76 N, 95.37 °W)	2009.04.21	10:00	0.40	7.50	7.29		HONO: LP-DOAS/5%;	
		11:00	0.59	6.02	7.77		NO ₂ : LP-DOAS /3%;	Wong et al. (2012)
		12:00	0.74	5.45	8.03		J(NO ₂): SAFS;	

		13:00	0.66	4.89	8.03	P _{unknown} : 10~20%.	
		14:00	0.51	5.45	7.76		
		15:00	0.57	5.91	7.18		
		10:00	0.05	6.04	5.84		
Colorado (40.05 °N, 105.00 °W)	2011.02.19- 2011.02.25	11:00	0.08	5.49	6.39	HONO: NI-PT-CIMS;	
		12:00	0.46	2.39	6.64	NO ₂ : a cavity ring-down spectrometer	
		13:00	0.37	1.55	6.39	(Wagner et al., 2011)/5%;	
		14:00	0.28	1.27	6.02	J(NO ₂): Filter radiometers.	
		15:00	0.22	1.47	5.22		
						HONO: LOPAP;	
Jülich (50.92 °N, 6.36 °E)	2003.07.29	noon	0.50	0.35	6.63	NO ₂ : Chemiluminescence analyzer equipped with a photolytic converter for NO ₂ to NO conversion;	
						J(NO ₂): derived from actinic flux spectra measured by a scanning spectroradiometer.	
		10:00	0.42	3.91	6.31	HONO: Wet chemical derivatization	
Paris (40.72 °N, 2.21 °E)	2009.07.09- 2009.07.27	11:00	0.38	3.42	7.76	(SA/NED), HPLC detection	
		12:00	0.52	3.14	8.08	(NitroMAC)/12%;	
		13:00	0.67	3.00	8.24	NO ₂ : Luminol chemiluminescence/5%;	
		14:00	0.38	3.00	7.29	J(NO ₂): filter radiometer/ 20–25%.	
		15:00	0.35	3.11	7.88		

	10:00	0.08	10.49	1.16
	11:00	0.11	10.49	1.80
2010.01.15-	12:00	0.18	9.44	2.60
2010.02.15	13:00	0.21	8.76	2.20
	14:00	0.20	9.12	2.34
	15:00	0.22	9.07	1.99

WD/IC: Wet Denuder sampling/Ion Chromatograph analysis system; TUV: Ultraviolet-Visible Model; TEI: Thermo Environmental Instruments; LOPAP: Long path absorption photometer; LP-DOAS: Long path Differential Optical Absorption Spectroscopy instrument; SAFS: scanning actinic flux spectroradiometer; NI-PT-CIMS: Negative-Ion Proton-Transfer Mass Spectrometer; SA/NED: an aqueous sulphanilamide/ N-(1-naphthyl)-ethylenediamine solution; NitroMAC: an instrument developed at the laboratory (Afif et al., 2014); HPLC: High Performance Liquid Chromatography.

Note that: Since $J(\text{NO}_2)$ data of Wu et al. (2012), N. Zhang et al. (2012), Zhou et al. (2002b), VandenBoer et al. (2013), Kleffmann et al. (2005) were not measured, they were calculated from the $J(\text{HONO})$ measurement data ($J(\text{NO}_2) = 5.3J(\text{HONO})$) (Kraus and Hofzumahaus, 1998); $J(\text{NO}_2)$ data of Zhou et al. (2002ab) were derived from the campaign of N. Zhang et al. (2012) (The experiments were conducted in summer and the studied sites were close to each other). $J(\text{NO}_2)$ data of Spataro et al. (2013) were also calculated from the $J(\text{HONO})$ at noon ($J(\text{NO}_2) = 5.3J(\text{HONO})$), then we computed the hourly $J(\text{NO}_2)$ (8:00~14:00 LST) through multiplying by the cosine of solar zenith angle. The NO_2 mixing ratios of N. Zhang et al. (2012) and Zhou et al. (2002b) were not shown and derived from NO_x mixing ratios. Similarly, NO_2 mixing ratios of Kleffmann et al. (2005) were inferred from NO mixing ratios.

References

- Elshorbany, Y. F., Kurtenbach, R., Wiesen, P., Lissi, E., Rubio, M., Villena, G., Gramsch, E., Rickard, A. R., Pilling, M. J., Kleffmann, J.: Oxidation capacity of the city air of Santiago, Chile. *Atmospheric Chemistry and Physics*, 9(6), 2257-2273, 2009.
- Hofzumahaus, A., Rohrer, F., Lu, K., Bohn, B., Brauers, T., Chang, C.C.: Amplified trace gas removal in the troposphere, *Science*, 324, 1702-1704, 2009.
- Kleffmann, J., Gavriloaiei, T., Hofzumahaus, A., Holland, F., Koppmann, R., Rupp, L., Schlosser, E., Siese, M., and Wahner, A.: Daytime formation of nitrous acid: a major source of OH radicals in a forest, *J. Geophys. Res. Lett.*, 32(5), doi: 10.1029/2005GL022524, 2005.
- Michoud, V., Colomb, A., Borbon, A., Miet, K., Beekmann, M., Camredon, M., Aumont, B., Perrier, S., Zapf, P., Siour, G., Ait-Helal, W., Afif, C., Kukui, A., Furger, M., Dupont, J. C., Haeffelin, M., Doussin, J. F.: Study of the unknown HONO daytime source at a European suburban site during the MEGAPOLI summer and winter field campaigns. *Atmospheric Chemistry and Physics*, 14(6), 2805-2822, 2014.
- Sörgel, M., Regelin, E., Bozem, H., Diesch, J. M., Drewnick, F., Fischer, H., Harder, H., Held, A., Hosaynali-Beygi, Z., Martinez, M., Zetzsch, C.: Quantification of the unknown HONO daytime source and its relation to NO₂, *Atmospheric Chemistry and Physics*, 11(20), 10433-10447, 2011.
- Spataro, F., Ianniello, A., Esposito, G., Allegrini, I., Zhu, T., Hu, M.: Occurrence of atmospheric nitrous acid in the urban area of Beijing (China), *Science of the Total Environment*, 447, 210-224, 2013.
- Su, H., Cheng, Y., Oswald, R., Behrendt, T., Trebs, I., Meixner, F. X., Andreae, M. O., Cheng, P., Zhang, Y., Pöschl, U.: Soil nitrite as a source of atmospheric HONO and OH radicals, *Science*, 333(6049), 1616-1618, 2011.
- Su, H., Cheng, Y. F., Shao, M., Gao, D. F., Yu, Z. Y., Zeng, L. M., Slanina, J., Zhang, Y. H., Wiedensohler, A.: Nitrous acid (HONO) and its daytime sources at a rural site during the 2004 PRIDE - PRD experiment in China, *Journal of Geophysical Research: Atmospheres* (1984–2012), 113(D14), 2008.
- VandenBoer, T. C., Brown, S. S., Murphy, J. G., Keene, W. C., Young, C. J., Pszenny, A. A. P., Kim, S., Warneke, C., de Gouw, J. A., Maben, J. R., Wagner, N. L., Riedel, T. P., Thornton, J. A., Wolfe, D. E., Dubé W. P., Öztürk, F., Brock, C. A., Grossberg, N., Lefer, B., Lerner, B., Middlebrook, A. M., Roberts, J. M.: Understanding the role of the ground surface in HONO vertical structure: High resolution vertical profiles during NACHTT-11. *Journal of Geophysical Research: Atmospheres*, 118, 10,155–10,171, doi:10.1002/jgrd.50721, 2013.
- Villena, G., Wiesen, P., Cantrell, C. A., Flocke, F., Fried, A., Hall, S. R., Hornbrook, R. S., Knapp, D., Kosciuch, E., Mauldin, R. L., McGrath, J. A., Montzka, D.,

- Richter, D., Ullmann, K., Walega, J., Weibring, P., Weinheimer, A., Staebler, R. M., Liao, J., Huey, L. G., and Kleffmann, J.: Nitrous acid (HONO) during polar spring in Barrow, Alaska: a net source of OH radicals?, *J. Geophys. Res. –Atmos.*, 116(D14), doi: 10.1029/2011JD016643, 2011.
- Wang, F., An, J., Li, Y., Tang, Y., Lin, J., Qu, Y., Cheng, Y., Zhang, B., Zhai, J.: Impacts of Uncertainty in AVOC Emissions on the Summer RO_x Budget and Ozone Production Rate in the Three Most Rapidly-Developing Economic Growth Regions of China, *Advances in Atmospheric Sciences*, 31, 1331–1342, 2014.
- Wu, J., Xu, Z., Xue, L., and Wang, T.: Daytime nitrous acid at a polluted suburban site in Hong Kong: indication of heterogeneous production on aerosol, in: *Proceedings of 12th international conference on atmospheric sciences and applications to air quality*, Seoul, Korea, 3–5 June 2013, 52, 2013.
- Wong, K. W., Tsai, C., Lefter, B., Haman, C., Grossberg, N., Brune, W. H., Ren, X., Luke, W., Stutz, J.: Daytime HONO vertical gradients during SHARP 2009 in Houston, TX, *Atmospheric Chemistry and Physics*, 12(2), 635-652, 2012.
- Zhang, Q., Streets, D. G., Carmichael, G. R., He, K., Huo, H., Kannari, A., Klimont, Z., Park, I., Reddy, S., Fu, J. S., Chen, D., Duan, L., Lei, Y., Wang, L., Yao, Z.: Asian emissions in 2006 for the NASA INTEX-B mission, *Atmospheric Chemistry and Physics*, 9, 5131-5153, 2009.
- Zhang, N., Zhou, X., Bertman, S., Tang, D., Alaghmand, M., Shepson, P. B., Carroll, M. A.: Measurements of ambient HONO concentrations and vertical HONO flux above a northern Michigan forest canopy. *Atmospheric Chemistry and Physics*, 12(17), 8285-8296, 2012.
- Zhou, X., Civerolo, K., Dai, H., Huang, G., Schwab, J., Demerjian, K. Summertime nitrous acid chemistry in the atmospheric boundary layer at a rural site in New York State, *Journal of Geophysical Research: Atmospheres* (1984–2012), 107(D21), ACH-13, 2002a.
- Zhou, X., He, Y., Huang, G., Thornberry, T. D., Carroll, M. A., and Bertman, S. B.: Photochemical production of nitrous acid on glass sample manifold surface, *Geophys. Res. Lett.*, 29, 26-1 – 26-4, doi: 10.1029/2002GL015080, 2002b.